

INFLUENCE OF TIN ADDITIONS ON MICROSTRUCTURE, MECHANICAL PROPERTIES AND SLIDING WEAR BEHAVIOUR OF Al-6.9%Si-1.7%Cu ALLOY

Muhammad A. Fakhri¹ & Israa A. Alkadir²

¹Department of Production Engineering and Metallurgy / University of Technology- Baghdad

Phone number: 0060111874033, Email address : alengmaf@gmail.com, muhd-al-jafar@outlook.com

ABSTRACT: *This research is devoted to study the effects of adding the alloying element Sn with different percentages (1, 3, 5) wt% on the microstructure, mechanical properties and dry sliding wear resistance of the Al-6.9wt%Si-1.7%Cu alloy. The microstructures are examined with an optical microscope for the base alloy and the alloy after said alloying element has been added. This experiment has revealed that changes have occurred on the morphology of grain as well as the precipitation of intermetallic compounds and other phases (Al_2Cu & $\beta-Sn$) determined by x-ray diffraction. A study is then conducted on the effects of alloying elements on mechanical properties (ultimate tensile strength, yield strength, percentage of elongation), hardness and impact toughness. The results show that the (σ_u , σ_y) and hardness decreased with increasing the percentage of Sn, but El% increased with increasing the weight percentage of Sn. Also we examined the impact toughness, and the results showed that the impact toughness after addition alloying element was lower than the base alloy. The pin-on-disk technique used to determine the wear resistance for base alloy and the alloy after adding alloying elements. The results show that the wear resistance increased with increasing the percentage of Sn at different applied loads (2.5, 5, 7.5)N with a constant sliding speed (3.7) m/sec.*

Keywords

Al-6.9%Si-1.7%Cu, microstructure, intermetallic compound, impact toughness, wear resistance

1. INTRODUCTION

Nowadays, engine blocks or gearbox housings, in addition to other components of modern transportation vehicles such as power trains and automotives, are considerably produced from recycled Al-Si alloys on high-pressure die-casting machines. This is a cost-efficient combination of material and process that is applicable for sustainable mass production [1]. That being said, there is an increasing demand for Al-Si cast alloys with better performance concerning yield and tensile strength. Such a trend is conjugated with weight reduction and requests to reduce exhaust emissions for automotive manufacturers as a major issue in this field. [2,3]. There are different phases in the Al-Si alloys that may lead to significant effects on the mechanical properties, positive and negative alike. The most visible phases, apart from the Al phase, are the Al-Si and Al-Cu phases, which play an important role to enhance the mechanical properties of Al-Si alloys, specifically the Al-Si-Cu alloy. Moreover, the brittle and resilient features of the silicon particles will lead to an increase in the ultimate tensile and yield of the softer aluminum matrix. Here, the lack in ductility in this alloy is probably due to the platelet-like features of Si particles.

Nevertheless, Al-Si cast alloys constitute up to 85-90% of cast aluminium (Al) products. Different elements are alloyed to Al-Si alloys as well. This is to further enhance the properties of Al-Si alloys, such as Carbon (C), Zinc (Zn), Lead (Pb), Tin (Sn), Indium (In), Cadmium (Cd), Magnesium (Mg), Copper (Cu), Ferum (Fe), Beryllium (Be), Manganese (Mn), Chromium (Cr), and Nickel (Ni). In general, Mg and Cu are the major alloying elements added to Al-Si alloys for precipitation-hardening [4]. Given the distinct properties for Al-Si-Cu alloys, such as high resistance against corrosion, stellar castability, depressed density, elevated productivity, low shrinkage rate and high strength comparing to weight ratio, those alloys are therefore used in the automotive industry on a large scale [5]. The accelerated need for weight reduction, however, leads to higher mechanical and thermal loading of these aluminum castings in future vehicles,

requiring improved Al-Si alloys. Therefore, in recent years, several investigations were carried out with the objective of improving the mechanical properties of Al-Si alloys [1]. Tin (Sn) is one of the minor alloying elements in Al alloys. In the past, it was added to increase the fluidity of casting alloys, and presently it is added to alloys for bearings [6].

Today Sn is a necessary component in a bearing because of its excellent anti-welding characteristics with iron, its low modulus and low strength. The addition of Sn to Al-Si alloys or Si to Al-Sn alloys can meet many of the requirements to attain an acceptable balance of strength and soft surface properties [7].

2. EXPERIMENTAL PROCEDURE

A. Casting process of alloys

Experimental alloys have been prepared using an electrical resistance furnace for melting purposes. The Al-Si-Cu alloy has been used as a master alloy with a chemical composition as listed in Table 1. Different percentages of Sn (small spherical shape bits) have been alloyed with the master alloy to give a chemical composition as listed in Table 2. The melting temperature is kept at $725 \text{ }^\circ\text{C} \pm 5 \text{ }^\circ\text{C}$; the molten metal is then degassed for 30 min using calcium flurid powder and argon gas. Sn bits are subsequently distributed depending on the proposed percentage for alloying and wrapped with a thin foil. After removing the slag from the molten alloy, the preheated Sn bits are added slowly to molten alloy by stirring with a coated and preheated mild steel plunger for 2-3 minutes at a speed of 300 rpm to enable complete dissolution and homogenization. The alloys are then cast into a preheated permanent mould in the form of cylindrical rods as shown in Fig (1). 5-10 minutes after pouring, the cast is removed out of the mould. The chemical composition of the master alloy and the alloy with additives are examined with an optical emission spectrometer (model: AMETEK materials analysis DIVI- ION). The specimens are prepared for the microstructure test and other mechanical tests by wet grinding with a grinder machine (model: MOPAO 160E) and emery paper of various grades (220,

320, 500, 1000 respectively) under running tap water, followed by polishing with a polishing machine (model: UNIPOL 820) with 5 μ m- and 0.5 μ m-alumina slurries in subsequent order. These specimens are then etched with Killer's solution (1ml HF+1.5ml HCL+ 2.5ml HNO3 +95ml distilled water). Specimens for microstructure and x-ray diffraction are thus prepared as per standard metallurgical procedures and photographed using computerized optical microscope model (BEL engineering metallographic microscopes model: MTM-1A).

B. Mechanical Tests

The mechanical properties of alloys are evaluated in terms of hardness, tensile strength, impact and wear resistance. The hardness of the samples is determined by using a Vicker's hardness-testing machine, where Vickers hardness number (VHN) is calculated from the equation number 1. The samples are of cylindrical shape at 20 mm in diameter and 10

mm in height. The applied load is 0.5 kgf in this test, with a dwell time of 15 seconds. Tensile tests are performed at room temperature on as-cast and grain refined specimens following the ASTM: E8/E8M-00b standard [8]. As shown in Figure 3. At least two samples were used for each set of tests. For the impact test, impact energy for samples is measured by using Charpy v-notched impact tests. The dimensions of standard Charpy test specimen according to the ASTM standard E23 [9]. The Pin-On-Disc machine is used to carry out the wear test experiment. A carbon steel disc is used as a counter face with a hardness of 35HRC. The disc rotational speed is at (510 RPM) with a linear sliding speed of (3.7) m/sec. The linear speed was calculated from equation number 2, while two formulas were used to convert the weight loss in to wear rate and to calculate the total sliding distance as described in equation3 & 4. Figure 2 provides a clear representation of the experimental procedure for this study.

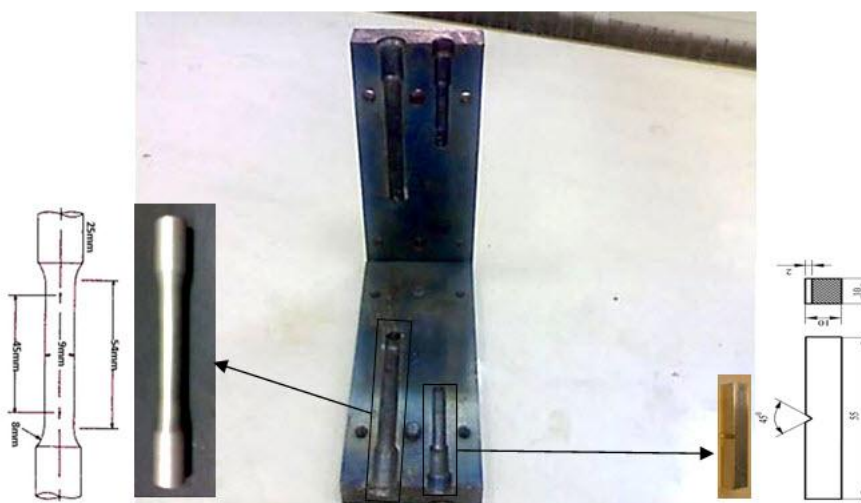


Figure 1. Casting design used in the experiments. The black boxes show the areas where the Charpy and tensile specimens were drawn.

Table (1) The chemical analysis of Al-Si alloy

Sample	Si%	Fe%	Cu%	Mn%	Mg%	Cr%	Ni%	Zn%	Ti%	Pb%	Sn%	V%	Al%
No1	6.92	1.721	0.496	0.122	0.043	0.022	0.101	0.947	0.127	0.039	0.025	0.007	Bal

Table (2) The chemical analysis of Al-Si alloy after addition alloying elements

Sample	Si%	Fe%	Cu%	Mn%	Mg%	Cr%	Ni%	Zn%	Ti%	Sn%	Pb%	V%	Al%
Sample 1	6.92	1.610	0.461	0.113	0.049	0.015	0.086	0.896	0.115	0.942	0.029	.003	Bal
Sample 2	6.84	1.683	0.456	0.119	0.033	0.018	0.090	0.903	0.121	2.720	0.033	.001	Bal
Sample 3	6.89	1.636	0.445	0.111	0.023	0.020	0.082	0.837	0.113	4.834	0.019	.005	Bal

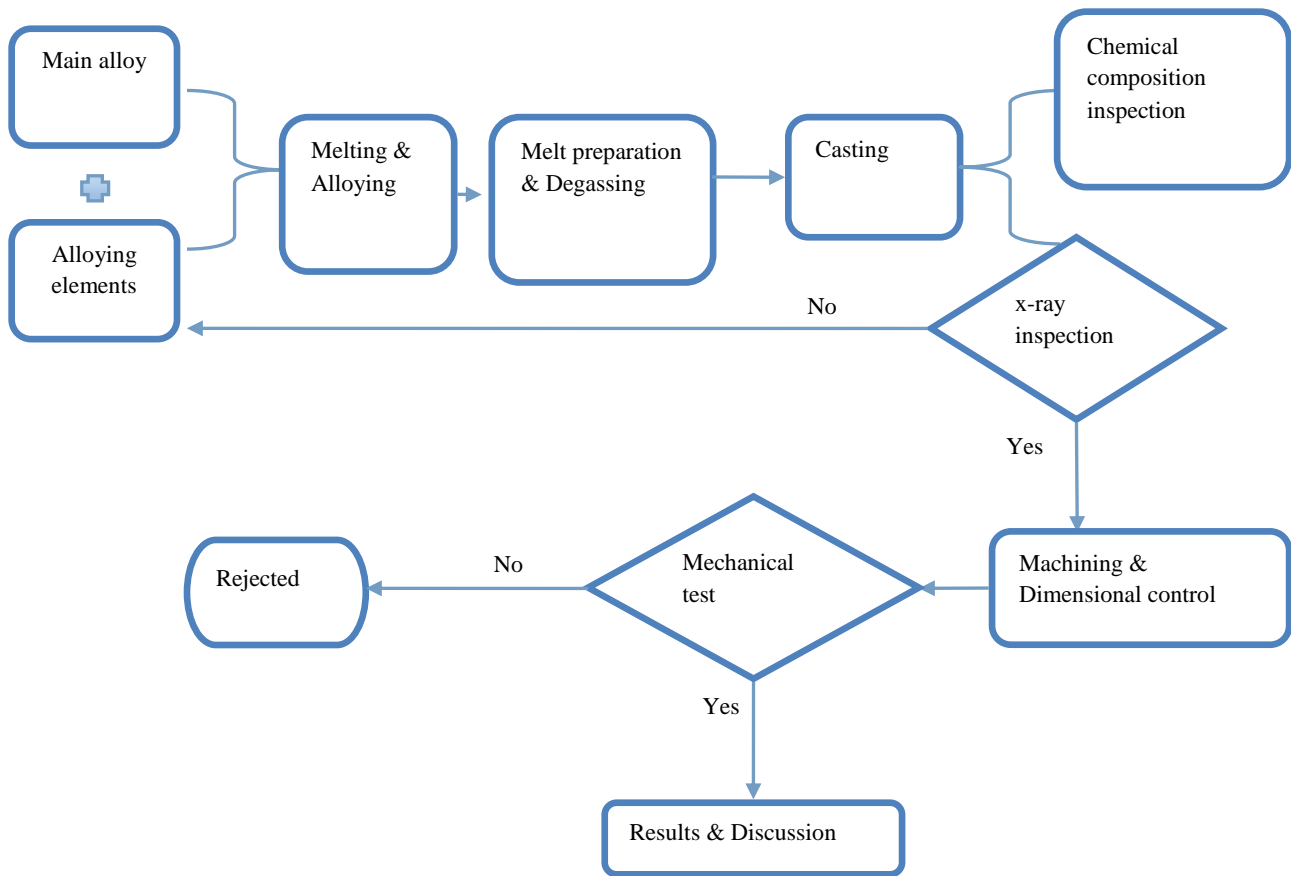


Figure 2. The experimental procedure.

$$VHN = 1.8544 \times \frac{P}{(d_{av})^2} \tag{1}$$

Where :-

- P = Applied load, kgf
- D = Average length of diagonals, mm
- HV = Vickers hardness Kg /mm²

$$V = \frac{\pi D_s N}{1000 \times 60} \tag{2}$$

where:-

- V = Linear sliding speed (m/sec)
- D_s = Sliding circle diameter (140) mm
- N = Disc rotational speed (510) RPM

Formula 3 used to convert the weight loss in to wear rate is :-

$$\text{Wear rate (weight loss)} = \frac{\Delta w}{s} \text{ (gm/cm)} \tag{3}$$

where:-

- Δw = Weight loss of the sample (gm)
- W₁ = Sample weight before the wear test (gm).
- W₂ = Sample weight after the wear test (gm).
- The total sliding distance (S) in cm was calculated as :-

$$S = V \times t \tag{4}$$

where:-

t = Running time (15 min) at each test.

3. RESULTS

A. Microstructure

Figure 3 shows the intermetallic phases that have been observed by x-ray diffraction examination, while the Figure 4 show the microstructures photographs that have been observed by an optical microscope of modified alloys. In Figure 3-d-, we observe different intermetallic phases such as (β-Sn, Al₂Cu), as well as the presence of such oxides as SiO₂ and SnO₂ in microstructure, where the appearance of those phases agrees with [5,6,10].

The photographs of microstructures obtained from computerized optical microscope are shown in Fig (4) for Al-6.9%Si-1.7%Cu with (1,3 and 5) % additions of Sn. Fig (4) a shows that the microstructure of the Al-6.9wt%Si-1.7wt%Cu alloy is α-Al and eutectic, thereby indicating that the structure has a dendritic shape. The addition of alloying elements (Sn) in different percentages of (1,3,5)wt% as shown in the same figures of b-d represents the changes that occur in the microstructure. These additions are responsible for the refining that has taken place in the α-phase and modification of eutectic structure. The alloys after Sn additions showed

that the Cu-containing phases, mainly Al₂Cu, nucleate either within the Al matrix or at the interface of such preexisting constituents as Si or intermetallic phases. The Cu phase occurs in block form as Al₂Cu, or as fine pockets of eutectic Al-Al₂Cu, addition to that the precipitation of Sn in the form of black reticulate particles of β(Sn). This phase is always

observed to precipitate within the Al₂Cu network (the white phases in the matrix are β(Sn) that precipitated within Al₂Cu network), attached to the Si particles. The distribution of the β(Sn) particles is not uniform, rather, they are distributed as small clusters[5,6,10].

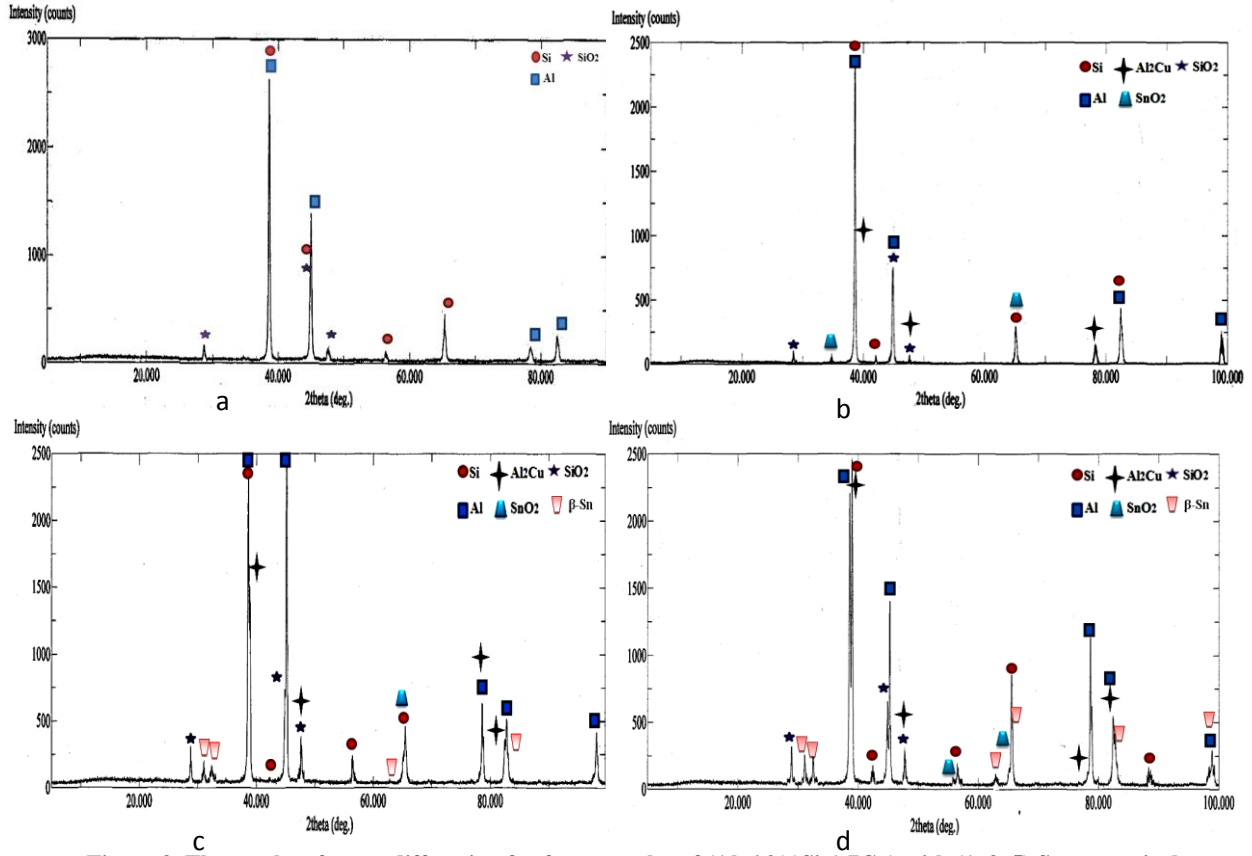
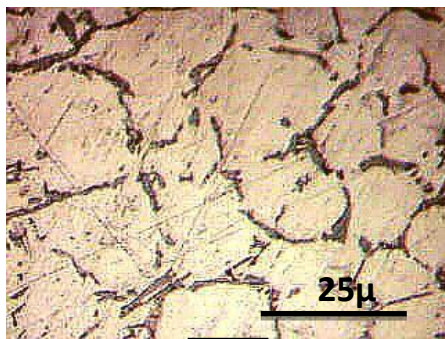
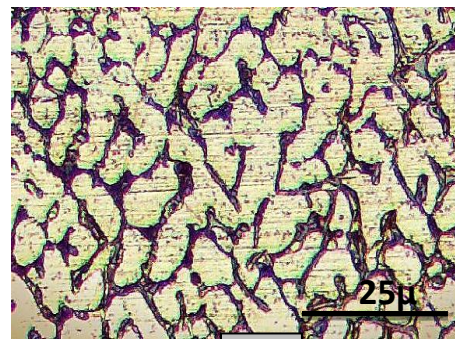


Figure 3. The results of x-ray diffraction for four samples of (Al-6.9%Si-1.7Cu) with (1, 3, 5) Sn respectively



(a)



(b)

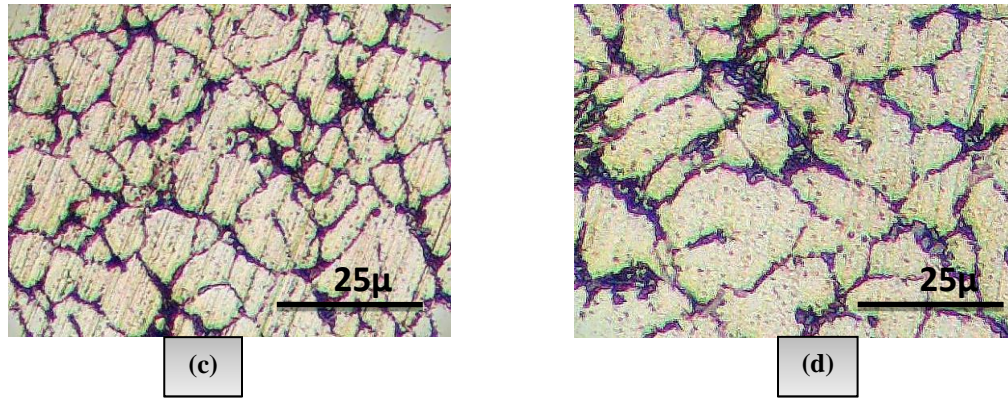


Figure 4. Optical micrographs of Al-6.9%Si-1.7%Cu and Al-Si-Cu-xSn alloys. (a) Al-6.9%Si-1.7%Cu, (b) Al-6.9%Si-1.7%Cu-1%Sn, (c) Al-6.9%Si-1.7%Cu-3%Sn, (d) Al-6.9%Si-1.7%Cu-5%Sn.

B-Tensile Examination

The following Figs (5 to 7) show the variation values of ultimate tensile strength, yield strength and elongation,

respectively, for Al-6.9% Si with different percentages of added Sn (1, 3, 5) wt.%.

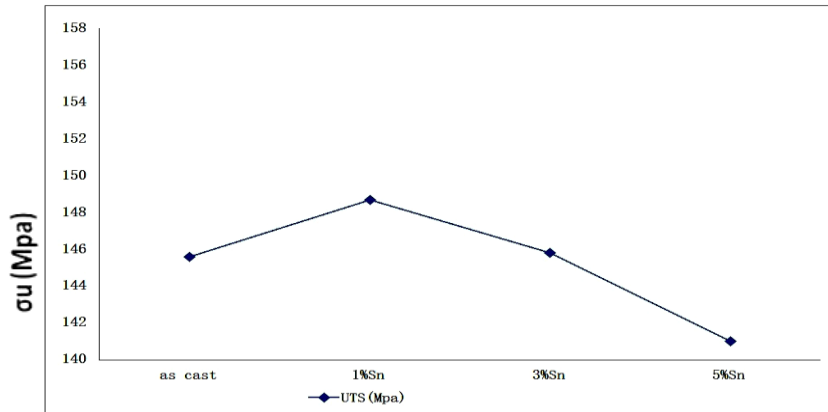


Figure 5. Relationship between Al-6.9%Si-1.7%Cu alloys with (1,3 & 5) wt%Sn and ultimate tensile strength(UTS).

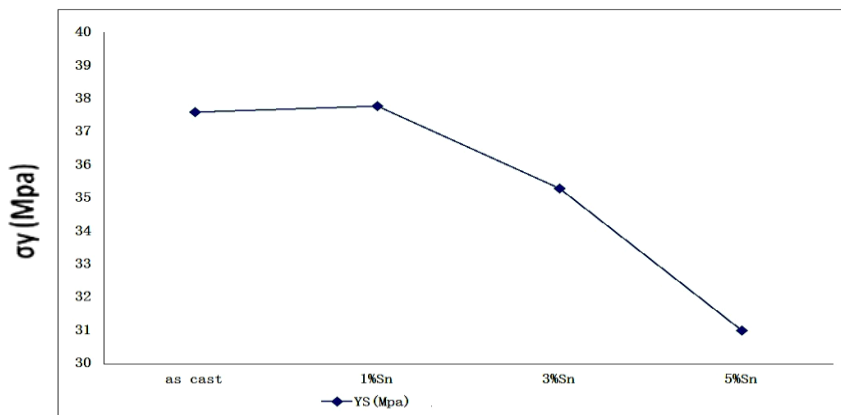


Figure 6. Relationship between Al-6.9%Si-1.7%Cu with(1,3 & 5) wt%Sn and yield strength (YS)

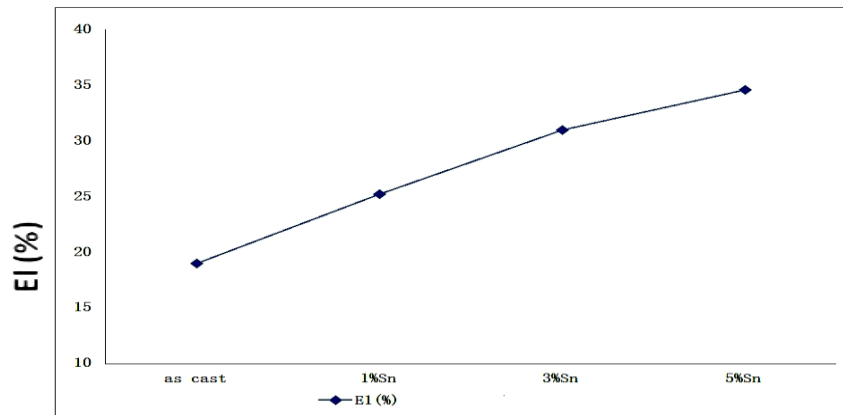


Figure 7. Relationship between Al-6.9%Si -1.7%Cu alloys with(1,3 &5) wt%Sn and elongation(EI)

For Fig (5) representing the relationship between ultimate tensile strength and weight percentages of Sn and Fig (6) representing the relationship between yield strength and weight percentages of Sn, the values of ultimate tensile strength (UTS) are obtained from curves and the yield strength (YS) computed by 0.2% offset method, according to ASTM standards E8M[11]. It is observed that 1 wt% Sn does not improve the tensile strength and yield strength too much, where it can be seen that the alloy with 1 wt% Sn has a tensile strength and yield strength 146.7 Mpa and 37.79 Mpa respectively while the original alloy has 145.6 Mpa and 37.6 Mpa respectively, this may be due to the puny effect of Sn on the original alloy when adding 1% wt of Tin—[12,13].

On the other hand the UTS and YS decrease with increase in weight percentage of Sn (3 and 5) %, because the increase in

weight percentage of Sn cause an increase in presence of β -Sn phase which act a soft phase [14,15]. Fig (6) shows that the ductility of all alloys increases with increasing the weight percentage of Sn because the increasing of β -Sn phase will increase the softening and grain size increase with increasing weight percentage of Sn additions [4].

C-Impact Examination

The impact tests of all samples are carried out with Charpy v-notched impact tests. The results are noted in the curves which have been drawn, as shown in Fig (8). The impact energy for the same alloys with 1%Sn and 3%Sn, but generally it still smaller than the base alloy, that can be due to the found of the β -Sn phase which be soft and cause the decrease in impact energy [6,12].

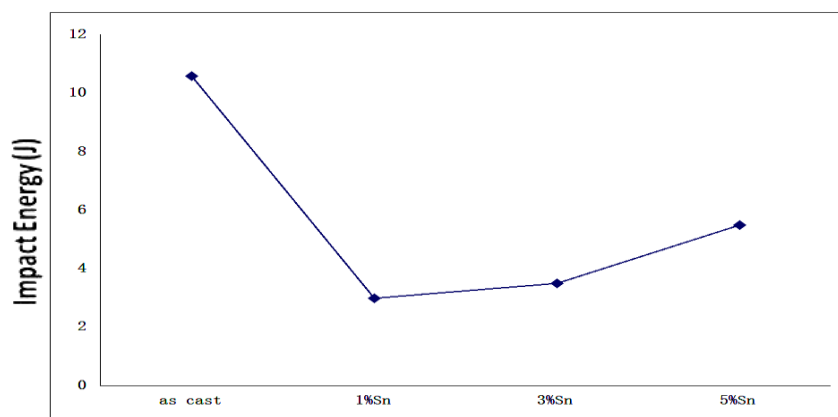


Figure 8. Relationship between Al-6.9%Si -1.7%Cu alloys with (1,3&5)wt%Sn and impact energy(IE)

D- Vicker's Hardness Examination

Fig (9) shows the variation values of Vickers hardness, for Al-6.9% Si with different percentage of additions Sn (1, 3, 5) wt.%. The macrohardness tests of the samples have been conducted using a Vicker's hardness test machine with a dwell time of 15 sec and applied load of 0.5 kgf (P) during the tests. For each composition, three indentations are taken and the average value is reported. Fig (9) shows the variation of

Vicker's hardness rate of Al-6.9wt % Si-1.7%Cu, with different percentages of added Sn (1, 3, 5) %. Vickers hardness values are found to be 55.125, 61.27, 59.8 and 58.35 respectively. This shows that hardness of the alloys increase with adding 1%Sn but it back to decrease with adding 3wt%Sn and 5wt%Sn. The decreases in hardness may be due to precipitate the large amount of β -Sn phase which be soft and causes the decrease in hardness [6, 12]

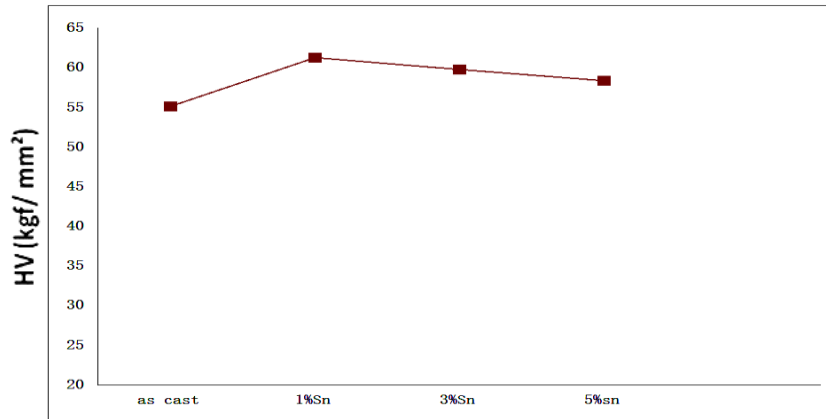


Figure 9. Relationship between Al-6.9%Si-1.7%Cu alloys with (1,3&5) wt%Sn and Vicker's hardness

E-Wear Examination

In this research three applied loads were used, (2.5,5,7.5) N in order to studying the effect of loads on wear resistance under constant sliding speed of 3.7 m/sec. Fig (10) shows that the wear rate increases with increase the load and weight percentage of Sn. The cause of increase in the wear rate at increasing of applied load is due to increasing plastic deformation at tip of the specimen surface – asperities. This can be explained by increase in the dislocation density and tiny increase in the hardness and brittleness of metal gradually. The dislocation condensation produces microvoids which join together to produce microcracks on the metal surface. These microcracks propagate under the effect of the applied load on the specimen surface at the direction of wear regions. Finally these cracks will connected with each other to produce big cracks as shown in Figs (11, 12& 13) which represent the surface topography of different worn surfaces for Al-Si-xSn under low and high loads under dry sliding conditions. Connection of these cracks together or with wear lines will lead to removing and separating of a thin layer from metal [6, 16]. This layer will be removed easily towards the sliding direction to produce wear debris particles which are generated by surface fatigue, at the surface layer during sliding process [17, 18].

The plastic deformation at the tip of asperities between sliding surface increases with the applied load, which causes increase in the real contact area. The adhesion between sliding surface asperities depends on the value and amount of

the applied load. When the applied load is small, a weak contact occurs at the tip of surface asperities only. During sliding this weak contact forms a thin oxide layer which acts as a protective surface film that covers the sliding surface and also protects direct metal contact between surface asperities is lower than the bonding force between metal atoms, this will produce a lower wear rate [16, 19]. When the applied load increases, fraction of the surface oxide layer may be detached, because of its brittleness it will be extruded outside the sliding surface of the specimen and disc during the sliding process. This produces metallic junction between the mating surfaces. The required shear force to shear the connected asperities is higher than the bonding force among the metal atoms themselves, this will lead to metallic particles separation from metal surface and finally increase in the wear rate [18, 20].

From Fig(10) it can be seen that the wear rate increase with increasing applied loads but it decrease with increasing the weight percentage of Sn this may be due to the Sn is a soft metal and generally used in babbitt alloys as a solid lubricant in plain bearings. The Sn metal solidifies along the grain boundaries of aluminum [19, 21]. This Sn provide an interface between the pin and wheel while sliding. As the pin wears the harder particulate is exposed, with the matrix eroding somewhat to provide a path for lubricant to flow between the rubbing surfaces. It provides an anti-frictional surface to reduce wear [22, 23].

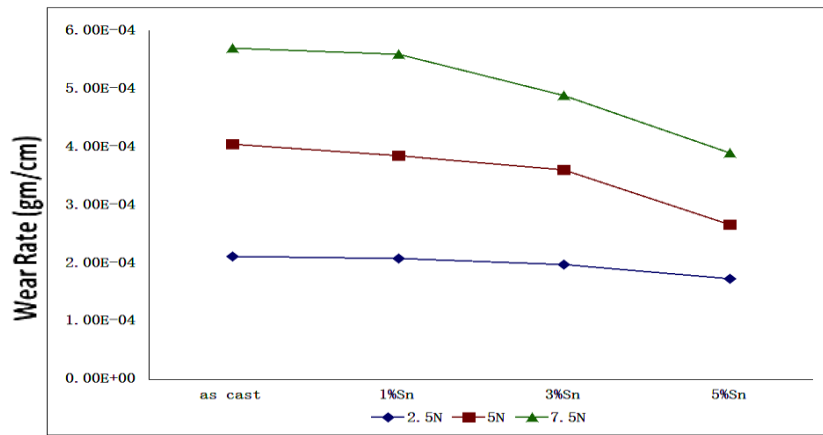


Figure 10. Relationship between Al-6.9%Si -1.7%Cu alloys with (1,3 & 5) wt%Sn and wear rate at constant sliding speed (3.7m/sec)

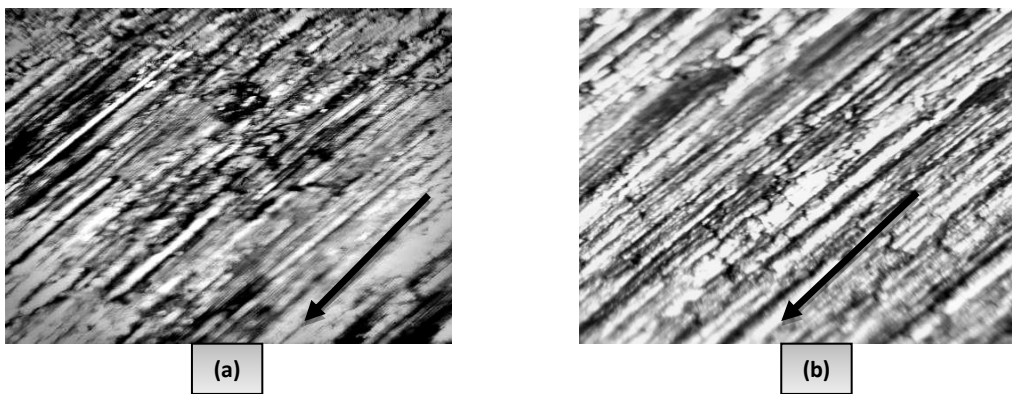


Figure 11. Optical micrographs of the surface topography of different worn surfaces under low and high loads of (2.5 and 7.5)N, under dry sliding conditions for Al-6.9%Si-1.7%Cu-1%Sn alloy, a- 2.5N, b- 7.5N at constant sliding speed(3.7m/sec).

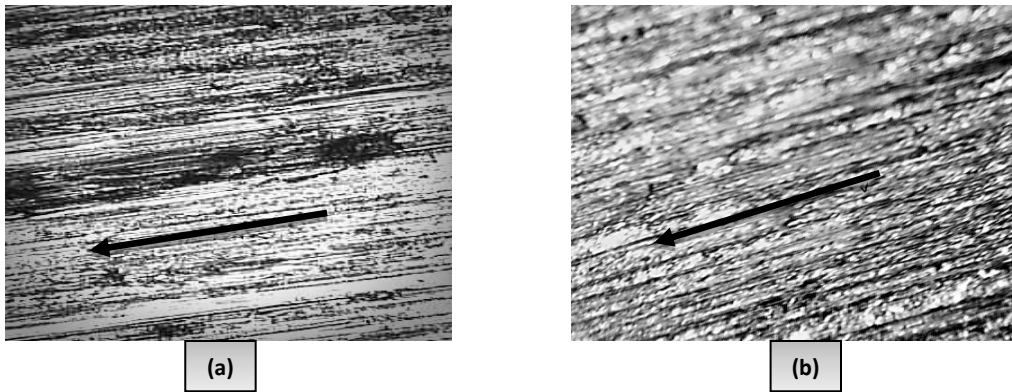


Figure 12. Optical micrographs of the surface topography of different worn surfaces under low and high loads of (2.5 and 7.5)N, under dry sliding conditions for Al-6.9%Si-1.7%Cu-3%Sn alloy, a- 2.5N, b- 7.5N at constant sliding speed (3.7m/sec).

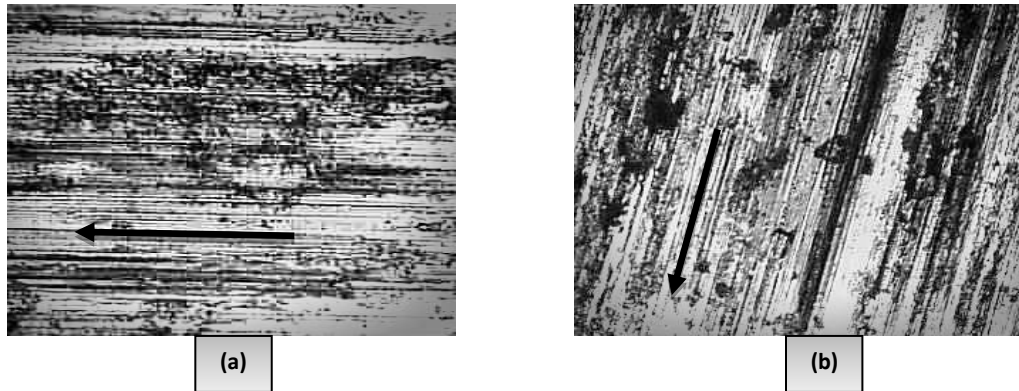


Figure 13. Optical micrographs of the surface topography of different worn surfaces under low and high loads of (2.5 and 7.5)N, under dry sliding conditions for Al-6.9%Si-1.7%Cu-5%Sn alloy, a- 2.5N, b- 7.5N at constant sliding speed (3.7m/sec).

4. CONCLUSIONS

Al-Si alloys have been widely adopted as debut materials for effectively facing environmental problems, and improving the fuel efficiency in the modern transportation vehicles such as power train and automotive.. These alloys are used due to their multiple features such as, reduced product weight, excellent cast ability, and high specific strength. The research aimed to study the effect of high additives level of Sn on the microstructure and mechanical properties of Al-Si-Cu alloy. The work included casting process for Al-Si-Cu alloy with three different percentages of Sn (1%, 3% and 5%), and microstructure and mechanical examinations of as-cast alloys and heat treated alloys to ensure the effect of each additive with different conditions. The results presented the improved properties as an outcome of certain percentage of additions, as well as the low properties. The summary of the conducted investigations are as follows:

The conclusions drawn from the conducted investigations are as follows:

1. The refining of the Si in eutectic structure and primary α with increasing on the weight percentage of Sn.
- 2- Total elongation increases with increasing the weight percentage of Sn.
3. Toughness, Yield strength and Ultimate Tensile strength decrease with increasing the weight percentage of Sn.
4. Hardness of Al-6.9%Si alloy decrease with the increase in amount of Sn present.
5. The wear resistance increases with increasing the weight percentage of Sn.

REFERENCES

- [1] Stadler.F, Antrekowitsch.H, Fragner.W, Kaufmann.H, Pinatel.E.R and Uggowitzer.P.J, " The effect of main alloying elements on the physical properties of Al-Si foundry alloys", Jo.of Materials Science and Engineering ,A560 ,pp.481-491, 2013 .
- [2] Forum, M. S., Fragner, W., Uggowitzer, P. J., & Zurich, E. T. H. The Effect of Ni on the High-Temperature Strength of Al-Si Cast Alloys, (January), 2016. <http://doi.org/10.4028/www.scientific.net/MSF.690.274>
- [3] Wong .Y .Ying, " investigation mechanical properties and microstructure of aluminum -silicon alloy using sand casting", Jo.of Faculty of Mechanical Engineering, pp4, 2010.
- [4] Hatch.J.E, "Aluminum: Properties and Physical Metallurgy", ed.,ASM, Metals Park, OH, pp. 50-51, 1984.
- [5] Samuel .F.H, Samuel .A.M and Doty .H.W, "Factors Controlling the Type and Morphology of Cu-Containing Phases in 319 Al Alloy" ,Jo.of AFS Transactions, Vol.104,pp.893-903, 1996.
- [6] Mohamed A.M.A, Samuel .F.H, Samuel .A.M, Doty .H.W and Valtierra .S, "Influence of Tin Addition on the Microstructure and Mechanical Properties of Al-Si-Cu-Mg and Al-Si-Mg Casting Alloys", Jo.of Metallurgical and Materials Transactions A, Vol. 39, pp.490-501, 2008.
- [7] Yuan.G.C, Li.Z.J, Lou.Y.X and Zhang.X.M, Jo.of Mater. Sci. Eng. A 280,108,2000.
- [8] (ASTM)E 8M – 00b, Standard Test Methods for Tension Testing of Metallic Materials, An American National Standard, 2000, Figure 8, pp 6.
- [9] ASTM E23 Standard Test Methods for Notched Bar Impact Testing of Metallic Materials.
- [10] Mulazimoglu .M.H, " Studies on the Minor Reactions and Phases in Strontium-treated Aluminum Silicon Casting Alloys", Jo.of Cast Metals, Vol. 6, pp. 16-28, 1993.
- [11] E8M-03, " tandard Test Method for Tension Testing of Metallic Materials(Metric)", A TM Annual Book of Standards West Conshohocken, Vol3, No1 PA, 2003.
- [12] Polmear .I.J, "Light Alloys: Metallurgy of the Light Metals", Jo.of Technology & Engineering , vol. 23, p. 117,1999.

- [13]Bolten. W, "Engineering Materials Technology," Butterworth's, Vol.3, 1998.
- [14] Xiaowu, Hu, Li Shuangming, Liu Lin, and Fu Hengzhi. "Microstructure Evolution of Directionally Solidified Sn-16 % Sb Hyperperitectic Alloy." (August): 167-7, 2008.
- [15] Qiu, Ke et al. "Effect of Individual and Combined Additions of Al-5Ti-B, Mn and Sn on Sliding Wear Behavior of A356 Alloy." *Transactions of Nonferrous Metals Society of China (English Edition)* 25(12): 3886-92, 2015. [http://dx.doi.org/10.1016/S1003-6326\(15\)64081-X](http://dx.doi.org/10.1016/S1003-6326(15)64081-X).
- [16] Israa .A.K, "The Effect of Lead Addition on the Wear Resistance of Al -16% Si Alloy Under Dry Sliding Conditions", *Jo.of Engineering and Technology* , Vol.24, No.1, pp.56-64, 2005.
- [17]Torabian .H, Pathak .J.P and Tiwari .S.N, "On Wear Characteristics of Lead Aluminum-Silicon Alloys" *Jo.of Wear*, Vol.77, pp. 47-54, 1994 .
- [18]Chaudhury. S.K. ,Singh. A.K ,Sivaramakrishnan.C.S and Panigrahi S.C,"Wear and Friction Behavior of Spray Formed and Stir Cast Al-2Mg-1TiO₂ Composites" ,*Jo .of Wear*, Vol. 258 (5-6, pp. 759-767), 2005.
- [19]Rashmi mittal and Devendra Singh," Dry sliding wear behaviour of spray formed ZrSiO₄ reinforced Al-Si-Sn alloy", *Adv. Mat. Lett*, No.3(1), pp.38-43, 2012.
- [20] Bolten. W, "Engineering Materials Technology," Butterworth's, 3rd ed, 1998.
- [21] Sahin.Y, "Wear Behaviour of Aluminium Alloy and its Composites Reinforced by SiC Particles using Statistical Analysis", *Jo. of Materials and Design*, Vol. 24, pp. 671-679, 2003.
- [22] Anli, M.; Srivastava, V.C.; Ghosh, M.K.; Ojha, S. N. *Wear* , 268, 1250, 2010.
- [23] Zhang. G.A and Wu.X.F , "Effect of Sn Addition on Microstructure and Dry Sliding Wear Behaviors of Hypereutectic Aluminum-Silicon Alloy A390", *Jo. of Materials Science*, Vol.46, pp. 7319-7327, 2011.